

Grain Size Effect on the Structural Parameters of the Stress Induced ϵ_{hcp} - Martensite in Iron-Based Shape Memory Alloy

Fabiana Cristina Nascimento^{a*}, Paulo Roberto Mei^b, Lisandro Pavie Cardoso^c, Jorge Otubo^d

^aDepartamento de Física, Universidade Federal do Paraná – UFPR, Rua Francisco H. dos Santos, Centro Politécnico, bloco II, CP 19081, 81531-990 Curitiba - PR, Brazil

^bFaculdade de Engenharia Mecânica, Universidade Estadual de Campinas – UNICAMP, Rua Mendeleiev, s/n, Cidade Universitária “Zeferino Vaz” Barão Geraldo CP 6122, 13083-970 Campinas, SP - Brazil

^cInstituto de Física Gleb Wataghin – IFGW, Universidade Estadual de Campinas – UNICAMP, Rua Mendeleiev, s/n, Cidade Universitária “Zeferino Vaz” Barão Geraldo, 13083-970 Campinas, SP - Brazil

^dInstituto Tecnológico de Aeronáutica – ITA, Praça Marechal Eduardo Gomes, 50, Vila das Acácias, 12228-900 São José dos Campos, SP - Brazil

Received: July 25, 2007; Revised: February 19, 2008

The aim of this work was to study the effect of austenitic grain size (GS) reduction on the structural parameters of the ϵ_{hcp} - martensite in stainless shape memory alloy (SMA). Rietveld refinement data showed an expansion in c-axis and a reduction in a and b-axis with thermo-mechanical cycles for all samples analyzed. Samples with $75 \leq \text{GS} (\mu\text{m}) \leq 129$ were analyzed. It was also observed an increase of the unit cell volume in this phase with GS reduction. The smallest grain size sample (GS = 75 μm) presented a c/a ratio of 1.649, and approximately 90% of total shape memory recovery.

Keywords: shape memory effect, stainless steel, rietveld refinement

1. Introduction

Iron-based shape memory alloys have been extensively studied in the last years due to their good shape recovery properties compared to other materials¹⁻¹². In stainless alloys, the shape memory effect (SME) is the result of a $\gamma(\text{fcc}) \leftrightarrow \epsilon(\text{hcp})$ martensitic transformation¹⁻³. The $\gamma(\text{fcc}) \rightarrow \epsilon(\text{hcp})$, $\gamma(\text{fcc}) \rightarrow \alpha'(\text{bcc})$ and $\gamma(\text{fcc}) \rightarrow \epsilon(\text{hcp}) \rightarrow \alpha'(\text{bcc})$ transformations can also occur and they depend on factors such as chemical composition and thermo-mechanical cycles. The forward and backward movements of Shockley partial dislocations on alternate {111} austenite planes promote the reverse $\epsilon(\text{hcp}) \rightarrow \gamma(\text{fcc})$ transformation resulting on the shape recovery of these materials^{4,7,9-13}. According to the literature^{4,7}, the thermo-mechanical treatment, chemical composition, and grain size (GS) reduction are some factors that have a strong influence on the SME, mechanical properties and structural parameters of austenitic and martensitic phases. In particular, the influence of GS on the shape recovery is a very important parameter to be studied, since some authors believe that the changes in austenitic grain size do not affect the shape recovery performance in stainless shape memory alloys¹⁴.

Recent works reported by our group^{7,13,15} showed that the GS reduction contributed to the increase of the total shape recovery (shape memory recovery + elastic recovery) and also it changed the mechanical properties in Fe-Mn-Si-Cr-Ni-(Co) SMA. Previous works have analyzed other properties and it was concluded that the grain size reduction improves the SMA in these alloys^{16,17}.

When the ϵ_{hcp} - martensite lattice parameters are associated to other parameters (such as mechanical properties) they can control the SME in stainless alloys. The literature states that an increase in the c/a ratio, strongly affected by chemical composition, makes the $\epsilon(\text{hcp}) \rightarrow \gamma(\text{fcc})$ transformation easier^{16,18}. This work is a complement to the data reported previously by our group^{7,13,15}, where we relate the structural changes of the martensitic phase to GS reduction, shape memory properties and thermo-mechanical cycles.

2. Experimental

The effects of GS reduction and thermo-mechanical cycles on the structural parameters of stress induced ϵ_{hcp} -martensite were analyzed for the following composition: Fe (balance) - 0.009 C - 8.26 Mn - 5.25 Si - 12.81 Cr - 5.81 Ni - 11.84 Co (wt%). The material was hot rolled at 1473 K followed by a heat-treatment at 1323 K for different times to obtain different austenite grain sizes samples⁷.

In order to induce the $\gamma(\text{fcc}) \leftrightarrow \epsilon(\text{hcp})$ martensitic transformation, the samples were submitted to six thermo-mechanical cycles (training). Each cycle consisted of 4% compression (to induce ϵ_{hcp} - martensite) and heating to 873 K during 30 minutes (to allow the shape recovery), and then cooling to room temperature. The specimen initial dimensions were 9 mm in length by 6 mm in diameter⁷.

The austenite average grain size was determined using optical microscopy. The specimen surface was mechanically polished and then etched with the solution: 2 mL HNO₃ + 2 mL NHCl in order to reveal the grain boundaries. To enhance the morphology of stress induced ϵ_{hcp} - martensite, the samples were electrolytic polished¹⁹. The color etching, K₂S₂O₅ + NH₄HF₂ in distilled water, was used to reveal the austenitic and martensitic phases²⁰. In this work, this etching was adapted for different GS and volume fraction ϵ_{hcp} - martensite^{7,19}.

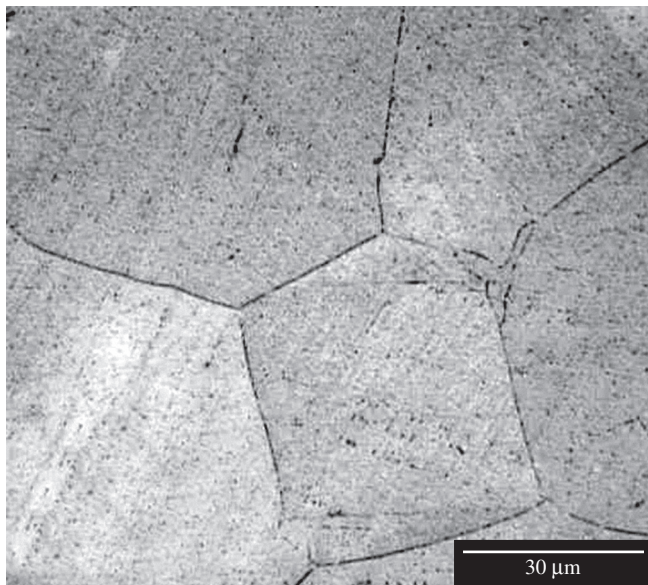
X ray diffraction (XRD) data were collected between 10 and 100° (2 θ) at room temperature using a Philips diffractometer (PW1710) with Cu target and a graphite diffracted beam monochromator, step sizes of 0.02° and 2 seconds of counting time. Structural parameters were analyzed by Rietveld method²¹ using the FullProf-suite software²². Peak shape, width parameters and background parameters were considered. All these parameters were refined adopting the iterative least-squares method through minimization of residual parameter. Two structure types were considered: a) cubic symmetry, space group **Fm-3m** for austenite phase, and b) hexagonal symmetry, space group **P6₃/mmc** ($\gamma = 120^\circ$) for the martensite phase. Lattice parameters correspond to a similar composition alloy, AISI-304 steel. The thermal parameters (B's) initially used for both phases were B_{overall} = 0.5 and the peak shape function used was the pseudo-Voigt.

*e-mail: fabiana.cristina@pesquisador.cnpq.br

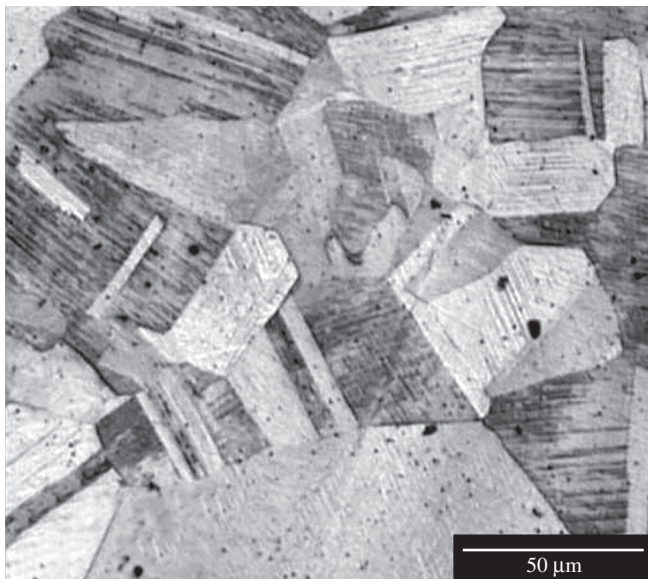
The mechanical^{4,7} and shape recovery^{7,15,19} properties presented here were obtained in our previous investigations.

3. Results and Discussion

The samples heated at 1323 K presented grain sizes between 75 and 129 μm . Before thermo-mechanical treatment cycles, the samples showed a whole austenitic matrix. The features showed in Figure 1a for GS = 106 μm were observed for all samples analyzed in this work. The average austenitic grain size was measured using similar images as the ones obtained in Figure 1a, where the grain boundaries revealed by the etching can be seen clearly, as explained in previous works^{19,23}. Stress induced ϵ_{hcp} - martensite started to appear with the



(a)



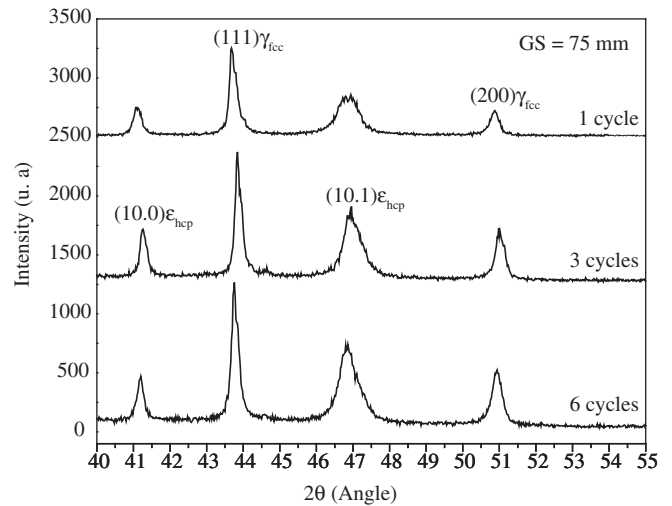
(b)

Figure 1. Optical microscopy: a) grain boundary of austenitic matrix, GS = 106 μm . Etchant: 2mHNO₃ + 2mNHCl, and b) stress induced ϵ_{hcp} - martensite (dark region) and γ_{fcc} - austenite (bright region), 6th thermo-mechanical cycle, GS = 75 μm . Color Etching: K₂S₂O₅ + NH₄HF₂ in distilled water¹⁹.

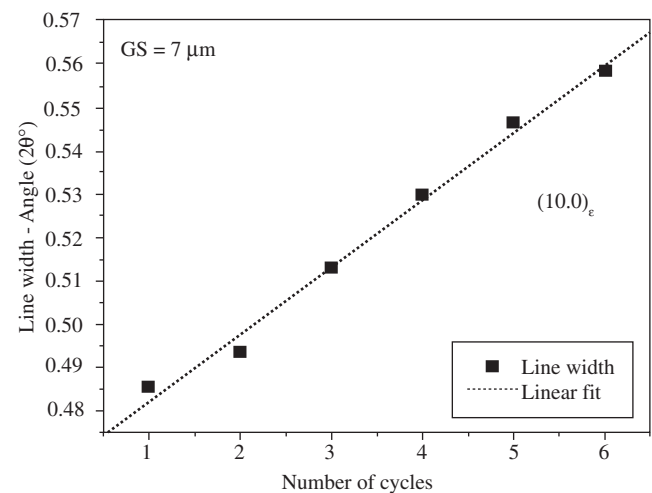
thermo-mechanical cycles. Figure 1b shows the optical microscopy of a sample with small grain size (GS = 75 μm), six thermo-mechanical cycles, and deformed state (no recovery). The band structure corresponded to the thin ϵ_{hcp} - martensite plates (dark region) distributed inside the austenitic grain (bright region). The samples with larger grain size have also presented a similar microstructure. The morphology of this phase was not affected by GS reduction and/or training cycles, remaining the band structure observed in Figure 1b.

Optical microscopy analysis of large GS samples has shown that a stress cycle ($\leq 2\%$) has induced α' - martensite (bcc-cubic symmetry and space group **Im-3m**). Several studies showed that this phase appears with the increase of the deformation or chemical composition^{9-11,13,18}. This phase was detected in regions of crossing plate ϵ_{hcp} - martensite in large grain size samples⁷. The α' (bcc) martensite formation is caused by double shear mechanism^{24,25} and was observed in large ϵ_{hcp} domains or intersections between several ϵ_{hcp} bands for similar compositions¹¹.

The effect of thermo-mechanical cycles on the ϵ_{hcp} - martensite was observed through X ray diffraction. Diffraction patterns of a sample with GS = 75 μm is shown in Figure 2a, deformed state, in



(a)



(b)

Figure 2. a) X ray diffraction patterns for 1st, 3rd and 6th thermo-mechanical cycles, deformed state, GS = 75 μm ; and b) Line width as a function number of cycle, (10.1) ϵ .

the range of $40^\circ \leq 2\theta \leq 55^\circ$ range, where there were more intense reflections. We have focused this work on this sample due to its 90% total shape memory recovery, which was previously presented in 15. In order to illustrate the training effect in Figure 2a, only the intermediary cycles were shown. Diffraction patterns of others cycles (2, 4 and 5) similar behavior. The most intense reflections for both phases were identified as: $(111)_\gamma$, $(200)_\gamma$, $(10.0)_\epsilon$ and $(10.1)_\epsilon$. The same peaks were detected in similar compositions by others authors using different radiation sources^{8,26,28}. Pronounced changes on the $\gamma(\text{fcc}) \rightarrow \epsilon(\text{hcp})$ transformation were observed for the $(111)_\gamma$ and $(10.1)_\epsilon$ peaks (Figure 2a). In this sample, the volume fraction increase of the martensitic phase with the number of cycles was detected through a change on the peak $(10.1)_\epsilon$. The linear increase of this peak line width is shown in Figure 2b. This result denotes the increasing on the volume fraction ϵ_{hcp} - martensite as a function of the number of cycles, a tendency observed in all samples. Particularly for this sample, the line width increased 15% between 1st and 6st cycles. For others grain size (106 and 129 μm) samples this difference was approximately 10%.

In this same diffraction range ($40^\circ \leq 2\theta \leq 55^\circ$) the Rietveld refinement of the first thermo-mechanical cycles, deformed state and small grain size, is shown in Figure 3. This figure presents the experimental and refined X ray diffraction patterns as well as their difference. All samples presented similar diffractions. The ϵ_{hcp} lattice parameters for the first cycle were: $a_{\epsilon(\text{hcp})} = 2.548(6)$ Å, $c_{\epsilon(\text{hcp})} = 4.162(2)$ Å, $c/a = 1.633(2)$, and they were larger when compared to the values presented in literature^{26,29}. Austenitic matrix indicated lattice parameters similar to the ones presented in the literature for stainless steel^{26,29}: $a_{\gamma(\text{fcc})} = 3.587(2)$ Å. Lattice parameters for the austenitic phase presented smaller variations (<3%). The standard deviations are shown in parenthesis. The discrepancies between the experimental and refined profiles for all samples are smaller, indicating that the unit cell dimensions were accurately determined and that the chosen peak shape function pseudo-Voigt was a good choice for these samples. The thermal parameters (B's) have presented a variation smaller than 0.5%.

The $\epsilon(\text{hcp})$ lattice parameters have changed as a function of the number of cycles (deformed state) for all grain sizes (Figure 4). It was observed a contraction on the a and b-axis with the number of cycles, while the c-axis expanded. For GS = 75 μm this increase was

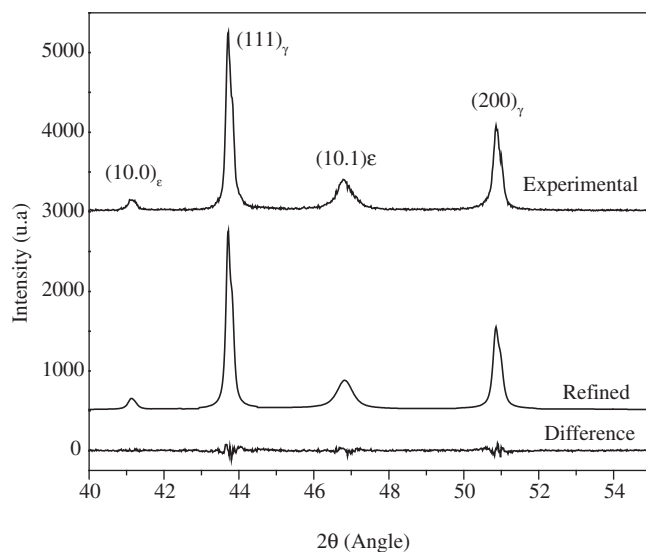


Figure 3. Rietveld refinement for GS = 75 μm , last thermo-mechanical cycle, deformed state.

approximately 0.50% between 1st and 6st cycles. The contraction observed in a and b-axis (same specimen) was smaller, 0.35% between the first and last cycles. In terms of grain size, the samples with refined microstructure presented an increase of all lattice parameters.

Grain size effect on the c/a ratio for all number of cycles is shown in Figure 5. In the last thermo-mechanical cycle, the sample with GS = 75 μm presented a $c/a = 0.70\%$, which was larger than the ratio for the sample with GS = 129 μm . This result, associated with other factors^{7,15} contributed to the improvement of shape recovery in this sample.

With the Rietveld refinement, it was possible to evaluate the grain size effect on the ϵ_{hcp} -martensite volume fraction of the intermediary thermo-mechanical cycles, deformed and recovered states (Figure 6). In the recovered state, the grain size reduction has facilitated the $\gamma(\text{fcc}) \rightarrow \epsilon(\text{hcp})$ transformation. This behavior was strengthened when the yield stress $\sigma_{0.2\%}$ was analyzed. In the work with a similar composition^{7,13} it was observed that the compressive yield stress decreased with the grain size. Therefore, the decrease in the $\sigma_{0.2\%}$ and the increase in the volume fraction of ϵ_{hcp} - martensite (Figure 6)

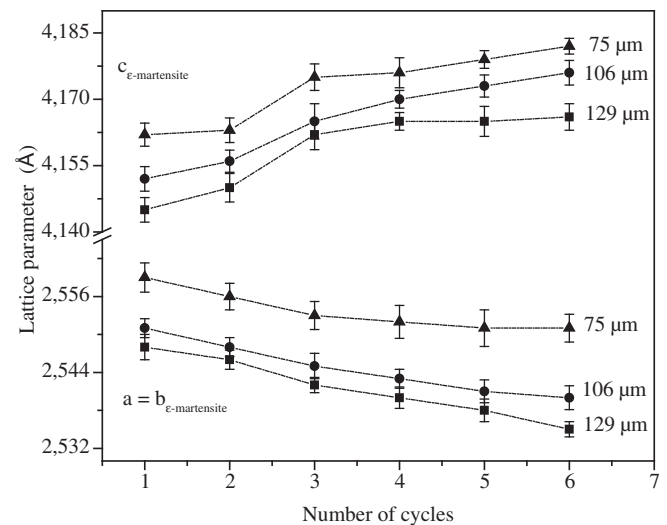


Figure 4. The ϵ (hcp) lattice parameter as a function number of cycles for different grain sizes.

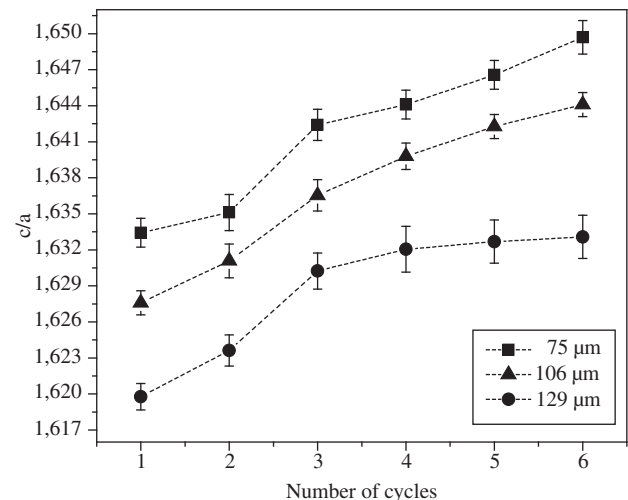


Figure 5. Grain size effect on the c/a ratio as a function number of cycles for different grain sizes.

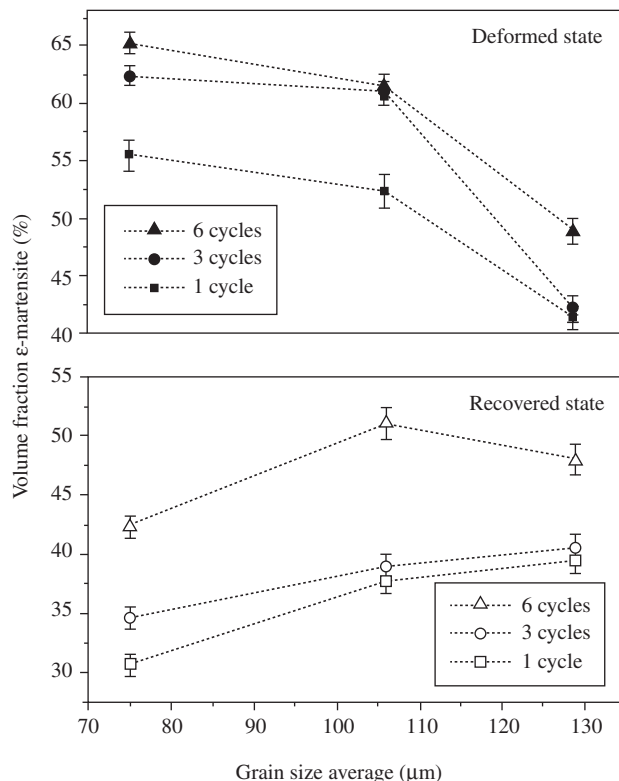


Figure 6. Volume fraction ϵ (hcp)-martensite as a function grain size for different number of cycles, deformed and recovered states.

show that this transformation is facilitated. GS reduction also has increased the amount of ϵ_{hcp} -martensite reversed ($\epsilon_{\text{hcp}} \rightarrow \gamma_{\text{fcc}}$) during the heating. In a similar composition¹³, this reversion was nearly complete. Corroborating with the previous results, the grain size reduction facilitated the $\epsilon_{\text{hcp}} \rightarrow \gamma_{\text{fcc}}$ transformation (Figure 6) where the sample with GS = 75 μm presented on the first cycle 50.9% martensite recovery⁷. This value decreased due to an accumulative process of martensite without recovery with number of cycles. Several factors contributed to facilitate the reverse martensitic transformation such as the increase of c/a ratio (expansion unit cell ϵ_{hcp} -martensite). In all thermo-mechanical cycles, the sample with GS = 75 μm presented a large c/a ratio, large volume fraction of reversed martensite and consequently, a large total shape recovery^{5,7}.

Improvements in shape recovery with c/a increase for different GS and number of cycles are shown in Figure 7. In this figure, it can be seen that the sample with $c/a = 1.646$, small GS at last cycle in a deformed state, presented a largest shape memory effect of 67.15%. With the increase of GS, this ratio decreased and corresponded to the condition of smallest SME.

The changes on the structural parameters detected by Rietveld refinement have shown a strong grain size influence presenting a relation with the shape memory recovery.

4. Conclusions

Grain size reduction effect in stainless SMA has promoted considerable changes on the structural parameters of martensitic phase. The expansion in the ϵ_{hcp} -martensite unit cell, detected by Rietveld refinement, increased the c/a ratio contributing thus, to increase the reversion of ϵ_{hcp} -martensite, and consequently, the shape memory recovery. For the thermo-mechanical cycles an expansion of the c -axis

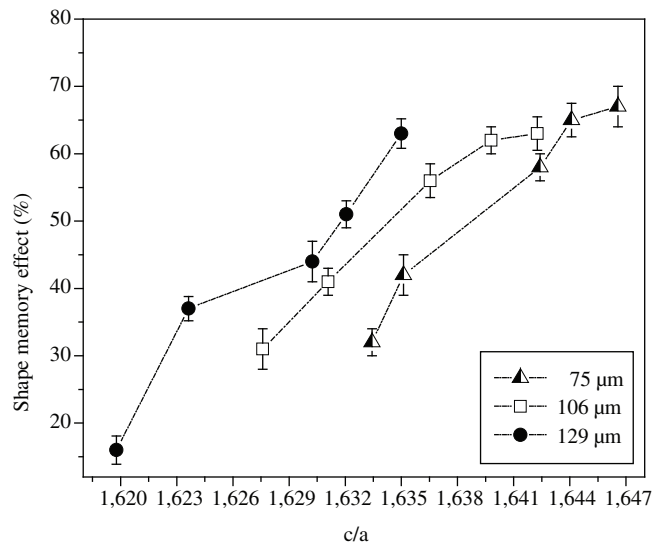


Figure 7. Shape memory recovery as a function of c/a for different grain size.

and the contraction of a and b -axis were detected. The sample with GS = 75 μm presented $c/a = 1.646$ in a last cycle at deformed state.

Acknowledgments

The authors would like to acknowledge FAPESP, CNPq, and UNICAMP for supporting the shape memory development project.

References

- Sato A, Chishima E, Soma K, Mori T. Shape memory effect in $\gamma \leftrightarrow \epsilon$ transformation in Fe-30Mn-1Si alloy single crystals. *Acta Metallurgica*. 1982; 30: 1177-1183.
- Sato A, Mori T. Development of a shape memory alloy Fe---Mn---Si. *Materials Science and Engineering A*. 1991; 146(1-2): 197-204.
- Otsuka H, Yamada H, Maruyama T, Tamahashi H, Matsuada S, Murakami M. Effects of Alloying Additions on Fe-Mn-Si Shape Memory Alloys. *ISIJ International*. 1990; 30(8): 674-679.
- Otubo J, Nascimento F C, Mei PR, Cardoso L P, Kaufman M. Influence of austenite grain size on mechanical properties of stainless shape memory alloy. *Materials Transactions JIM*. 2002; 43(5): 916-919.
- Christian, JW. A theory of the transformation in pure cobalt. Proceedings of the Royal Society of London. Seires A, Mathematical and Physical Sciences. 1951; A203(1084): 51-64.
- Seeger A. Versetzungen und allotrope umwandlungen. *Zeitschrift für Metallkunde*. 1953; 44: 247-255.
- Nascimento FC. *Efeito do tamanho de grão nas propriedades mecânicas e na recuperação de forma de ligas inoxidáveis com efeito de memória de forma*. [Thesis] Campinas, Brazil: Unicamp; 2002; p. 01-138.
- Jang WY, Gu Q, Van Humbeeck J, Delay L. Microscopic observation of γ -phase and ϵ - and α' -martensite in Fe-Mn-Si-based shape memory alloys. *Materials Characterization*. 1995; 34: 67-72.
- Bergeon N, Guenin G, Esnouf C. Characterization of the stress-induced ϵ -martensite in a Fe-Mn-Si-Cr-Ni shape memory alloy: microstructural observation at different scales, mechanism of formation and growth. *Materials Science and Engineering A*. 1997; 238: 309-316.
- Bergeon N, Guenin G, Esnouf C. Microstructural of the stress-induced ϵ -martensite in a Fe-Mn-Si-Cr-Ni shape memory alloy: Part I- calculate description of the microstructure. *Materials Science and Engineering A*. 1998; 242: 77-86.

11. Bergeon N, Guenin G, Esnouf, C. Microstructural of the stress-induced ϵ martensite in a Fe-Mn-Si-Cr-Ni shape memory alloy: Part II-Transformation reversibility. *Materials Science and Engineering A*. 1998; 242: 87-95.
12. Li H, Dunne D, Kennon N. Factors influencing shape memory effect and phase transformation behaviour of Fe-Mn-Si based shape memory alloys. *Materials Science and Engineering A*. 1999; 273-275: 517-523.
13. Otubo J, Mei PR, Shinohara AH, Suzuki CK, Koshimizu S. Relations between thermomechanical treatment, microstructure and α' martensite in Fe based stainless shape memory alloys. *Materials Science and Engineering A*. 1999; 273: 533-537.
14. Murakami, M., Suzuki, H., Nakamura, Y. Effect of Si on the shape memory effect of polycrystalline Fe-Mn-Si alloys. *Materials Transactions*. 1987; 27: 87-96.
15. Nascimento FC, Mei PR, Otubo, J. Effects of grain size on the shape recovering properties of a stainless SMA. In: *Proceedings of Conference Advances in Materials and Processing Technologies*, Las Vegas. 2003; 1436-1440.
16. Sato A, Matsuya T, Morishita M, Kumai S, Inoue A. Strengthening of Fe-Mn-Si based shape memory alloys by grain size refinement. *Shape Memory Materials*. 2000; 223-226.
17. Matsuya T, Yoneyama N, Kumai S, Sato A. Grain size effect on the microstructure of deformed Fe-Mn-Si based shape memory alloys. *Shape Memory Materials*. 2000; 323(3): 267-270.
18. Airapour A, Yakubtsov I, Perovic D D. Effect of nitrogen on shape memory effect of a Fe-Mn-based alloy. *Materials Science and Engineering A*. 1999; 262: 39-49.
19. Nascimento FC, Sorrila FV, Otubo J, Mei PR. Stainless shape memory alloys microstructure analysis by optical microscopy using different etchants. *Acta Microscopica*. 2003; 12(1): 99-105.
20. Gu Q, Humbeeck V, Delaey L, Guénin G, Gex D. Effect of amount of deformation on the martensitic transformation and shape memory effect in Fe-Mn-Si based shape memory steel. *Journal de Physique IV*. 1995; 5: 311-315.
21. Rietveld HMA profile refinement method for nuclear and magnetic structures. *Journal of Applied Crystallography*. 1969; 2: 65-71.
22. Carvajal JR. *An introduction to the program FullProf*. Laboratoire Léon [Manual] Brillouin, França, 2000 (Versão julho 2001).
23. Bueno JC, Nascimento FC, Mei PR, Otubo J. Stress induced martensite morphology in stainless shape memory alloys. *Acta Microscopica*. 2003; 12: 223-224.
24. Venables JA. Nucleation + propagation of deformation twins. *Philosophical Magazine*. 1964; 25(7): 693-695.
25. Fujita H, Katayama T. In-situ Observation of Strain-Induced $\gamma \rightarrow \epsilon \rightarrow \alpha'$ and $\gamma \rightarrow \alpha'$ Martensitic Transformations in Fe-Cr-Ni Alloys. *Materials Transactions JIM*. 1992; 33(3): 243-252.
26. Gauzzi F, Montanari R. Martensite reversion in an Fe-21%Mn-0.1%C alloy. *Materials Science and Engineering A*. 1999; 273-275: 524-527.
27. Chanda A, Pal H, De M, Kajiwarra S, Kikuchi T. Characterization of microstructure of isothermal martensite formed at low temperature in powder of Fe-23Ni-3.3Mn alloy by Rietveld method. *Materials Science and Engineering A*. 1999; 265: 110-116.
28. Jee KK, Baik SH, Lee BJ, Shin MC, Choi CS. Jee KK et al. Measurement of volume fraction of stress-induced ϵ martensite in Fe₃₂Mn₆fSi alloy. *Scripta Metallurgica at Materialia*. 1995; 33(12): 1901-1905.
29. Qingsuo L, Shihong M, Naju G. The $\gamma \rightarrow \epsilon$ -martensitic transformation and its reversion in the FeMnSiCrNi shape-memory alloy. *Metallurgical and Materials Transactions A*. 1998; 29A: 1579-1583.
30. Sahu P, De M, Kajiwarra, S. Microstructural characterization of stress-induced martensites evolved at low temperature in deformed powders of Fe-Mn-C alloys by the Rietveld method. *Journal of Alloys and Compounds*. 2002; 346(1-2): 158-169.

